Fizika Nizkikh Temperatur, 2010, v. 36, No. 7, p. 776–781

Theoretic specific heat from spin wave in comparison with experimental results in Fe-oxide superconductors

Li Jun[1], Zhang Yu-Feng[2], Qin Zhi-Jie[1], Niu Xiao-Li[1], Li Dong-Sheng[1], and Li Ping-Lin[1]

[1]*School of Physics and Engineering, Zhengzhou University, Zhengzhou 450052, China*

[2]*Shanghai University of Electric Power, Shanghai 200090, China*

E-mail: lipinglin@zzu.edu.cn

Received June 23, 2009, revised March 13, 2010

Based on the magnetic order of Fe-oxide superconductors from the experiments, we will apply Heisenberg interaction model and analyze systematically the antiferromagnetic configuration with the spin-density-wave, through the strictly mathematical-physical derivation, to suggest the analytic expressions of internal energy and specific heat under the long-wave conditions. The theoretic values show good consistence with the experiments, and both theoretic and experimental results are discussed sufficiently through the phonon contribution to the specific heat, therefore, the spin density wave theory can properly describe the physical characteristics of Fe-oxide superconductors.

PACS: **74.70.–b** Superconducting materials other than cuprates;
74.72.–h Cuprate superconductors;
75.10.–b General theory and models of magnetic ordering;
75.25.–j Spin arrangements in magnetically ordered materials.

Keywords: Fe-oxide superconductor, spin-density-wave, theoretic specific heat.

1. Introduction

The recent discovery of Fe-oxide superconductors with a remarkable T_c = 26 K in $LaO_{1-x}F_xFeAs$ [1] is a surprise to the scientific community. Afterwards, T_c was pushed up surprisingly to above 40 K on either applying pressure [2] or replacing La by Sm [3], Ce [4], Nd [5] and Pr [6]. The maximum T_c has climbed to 56 K, observed in $SmO_{1-x}F_xFeAs$ [7,8] and $SmO_{1-x}FeAs$ [9]. These iron arsenides have a layered structure like cuprates, and the superconducting electron pairing is believed to happen in the iron-based layers [10]. The pure LaOFeAs itself has not the superconductivity but shows an anomaly near 150 K in both resistivity and dc magnetic susceptibility [11].

The high transition temperature and the preliminary band structure calculation suggest that the superconductivity in these Fe-oxide superconductors is not mediated by electron–phonon interaction. By the first principles calculations, many scholars have studied the electronic and magnetic structures of LaOFeAs [12,13]. In the ground state, these local Fe moments are in the collinearly antiferromagnetic order, from which the interactions between the strong nearest- and next nearest-neighbor superexchange are bridged by As atoms [14]. Many studies suggest that the antiferromagnetic fluctuation plays an important role and sheds light on the comprehension of the pairing mechanism in Fe-oxide superconductors. Furthermore, the narrow superconducting phase from the spin-density-wave (SDW) instability implies that the magnetic fluctuation plays even a vital role in the superconducting pairing mechanism. The experimental and theoretical evidences exhibit that the evolution of SDW state with electron Nematic order induces the superconductivity in lower temperature [4,11].

The superconductivity occurs only in lower temperature, which reveals the close relationship between the superconductivity and the superconductor thermodynamic properties. Here, we suggest the analytic expressions of internal energy and specific heat under the long-wave conditions in Fe-oxide superconductors, from which the experimental magnetic order we apply Heisenberg interaction model and analyze systematically the antiferromagnetic configuration with the SDW through the strictly mathematical-physical derivation. Our analytic values show good consistence with the experimental results, therefore, the spin density wave theory can properly describe the physical characteristics of Fe-oxide superconductors.

2. Magnetic order and modeling

The crystal lattice in Fe-oxide superconductors is a square *p*4/*mm* symmetric layered structure as high-T_c cuprate superconductors [15]. All atoms line along *c* axis and make up one crystal cell with Fe–As and La–O layers appearing alternatively. As shown in Fig. 1, in the calculations we choose the experimental lattice constants a = = 4.03552 Å, c = 8.73930 Å [16] and adopt the SC layered Heisenberg model [17,18]. Here we introduce the $\sqrt{2}a \times \sqrt{2}a \times c$ crystal cell.

Suppose the interaction parameters concerning nearest- and next-nearest-neighboring between the magnetic moments in the antiferromagnetic configuration are J_1 and J_2, respectively (J_1, $J_2 > 0$). Hamiltonian H is expressed by spin operators $\hat{S}_i$ as follows:

$$H = \sum_{i,\,\delta} J_1 \hat{S}_i \hat{S}_{i+\delta} + \sum_{i,\,\varepsilon} J_2 \hat{S}_i \hat{S}_{i+\varepsilon}, \tag{1}$$

where i is lattice label; δ and ε, respectively, denote nearest and next-nearest-neighboring lattice point vectors. The first item after the equal sign is the nearest-neighboring summation and the second is next-nearest-neighboring summation. We can get Hamiltonian in terms of z component spin on up-down operators $\hat{S}^{\pm}$ and then introduce Dyson–Maleev approximate transformation [19,20]:

$$H = \sum_{i,\delta} J_1 \left\{ \hat{S}_i^z \hat{S}_{i+\delta}^z + \frac{1}{2}\left(\hat{S}_i^+ \hat{S}_{i+\delta}^- + \hat{S}_i^- \hat{S}_{i+\delta}^+ \right) \right\} +$$

$$+ \sum_{i,\varepsilon} J_2 \left\{ \hat{S}_i^z \hat{S}_{i+\varepsilon}^z + \frac{1}{2}\left(\hat{S}_i^+ \hat{S}_{i+\varepsilon}^- + \hat{S}_i^- \hat{S}_{i+\varepsilon}^+ \right) \right\}, \tag{2}$$

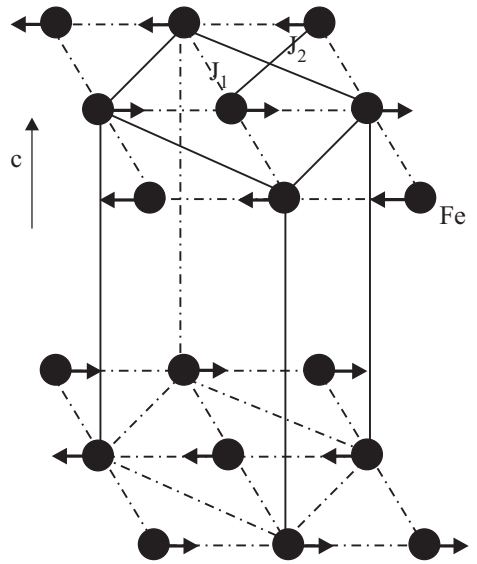

Fig. 1. Schematic diagram of magnetic order structures in the unit cell, the arrowhead denotes the direction of Fe ion's spin.

$$\hat{S}_i^z = S - a_i^+ a_i, \quad \hat{S}_i^+ = \sqrt{2S}\, a_i, \quad \hat{S}_i^- = \sqrt{2S}\left(a_i - \frac{a_i^+ a_i^+ a_i}{2S} \right),$$

$$\hat{S}_{i+\delta}^z = b_{i+\delta}^+ b_{i+\delta} - S, \quad \hat{S}_{i+\delta}^+ = \sqrt{2S}\, b_{i+\delta}^+,$$

$$\hat{S}_{i+\delta}^- = \sqrt{2S}\left(b_{i+\delta} - \frac{b_{i+\delta}^+ b_{i+\delta} b_{i+\delta}}{2S} \right), \quad \hat{S}_{i+\varepsilon}^z = b_{i+\varepsilon}^+ b_{i+\varepsilon} - S,$$

$$\hat{S}_{i+\varepsilon}^+ = \sqrt{2S}\, b_{i+\varepsilon}^+, \quad \hat{S}_{i+\varepsilon}^- = \sqrt{2S}\left(b_{i+\varepsilon} - \frac{b_{i+\varepsilon}^+ b_{i+\varepsilon} b_{i+\varepsilon}}{2S} \right). \tag{3}$$

All in Eq. (3) are applied in Eq. (2), and neglect the fourth-order items of all a and b operators, we get the approximate Hamiltonian in lower temperature T:

$$H = -NAJ_1 S^2 + \sum_{i,\delta} AJ_1 S(a_i^+ a_i + b_{i+\delta}^+ b_{i+\delta}) +$$

$$+ \sum_{i,\delta} J_1 S(a_i b_{i+\delta} + a_i^+ b_{i+\delta}^+) - NAJ_2 S^2 +$$

$$+ \sum_{i,\varepsilon} AJ_2 S(a_i^+ a_i + b_{i+\varepsilon}^+ b_{i+\varepsilon}) + \sum_{i,\varepsilon} J_2 S(a_i b_{i+\varepsilon} + a_i^+ b_{i+\varepsilon}^+). \tag{4}$$

Here N is the spin number in the lattice, and A is the coordinate number of the lattice. The above formula is consistent with the introduced Holstein–Primakoff approximate transformation [21,22].

3. Solution to *H* model

To solve Eq. (4), perform Fourier transformation and introduce spin wave operators a_k, b_k:

$$a_i = N^{-1/2} \sum_k \mathrm{e}^{i\mathbf{k}\mathbf{R}_i} a_k, \quad a_i^+ = N^{-1/2} \sum_k \mathrm{e}^{-i\mathbf{k}\mathbf{R}_i} a_k^+,$$

$$b_{i+\delta} = N^{-1/2} \sum_k \mathrm{e}^{-i\mathbf{k}\mathbf{R}_{i+\delta}} b_k, \quad b_{i+\delta}^+ = N^{-1/2} \sum_k \mathrm{e}^{i\mathbf{k}\mathbf{R}_{i+\delta}} b_k^+,$$

$$b_{i+\varepsilon} = N^{-1/2} \sum_k \mathrm{e}^{-i\mathbf{k}\mathbf{R}_{i+\varepsilon}} b_k, \quad b_{i+\varepsilon}^+ = N^{-1/2} \sum_k \mathrm{e}^{i\mathbf{k}\mathbf{R}_{i+\varepsilon}} b_k^+, \tag{5}$$

where $\mathbf{R}_i$, $\mathbf{R}_{i+\delta}$, $\mathbf{R}_{i+\varepsilon}$ denotes the vectors of lattice i, $i+\delta$ and $i+\varepsilon$, respectively. They are applied to Eq. (4):

$$H = -NA(J_1 + J_2)S^2 + AS \sum_k (J_1 + J_2)(a_k^+ a_k + b_k^+ b_k) +$$

$$+ AS \sum_k (J_1 \gamma_k + J_2 \gamma_k')(a_k b_k + a_k^+ b_k^+). \tag{6}$$

The first item is the energy of initial state, the second item is the sum of spin wave at each lattice, and the third item is the total interaction of spin wave. γ_k and γ'_k are the structure factors of spin wave, which satisfy the following relations, respectively:

$$\gamma_k = A^{-1}\sum_{\delta} e^{ik\delta} = \gamma_{-k}, \quad \gamma'_k = A^{-1}\sum_{\varepsilon} e^{ik\varepsilon},$$

$$\sum_k \gamma_k = A^{-1}\sum_{\delta\neq 0}\sum_k \frac{1}{A} e^{ik\delta} = 0, \qquad \sum_k \gamma'_k = 0. \tag{7}$$

Based on the Bogoliubov transformation, we introduce the combined spin wave operator to eliminate the cross item and perform H diagonalization:

$$\alpha_k = u_k a_k - v_k b_k^+, \quad \alpha_k^+ = u_k a_k^+ - v_k b_k,$$

$$\beta_k = u_k b_k - v_k a_k^+, \quad \beta_k^+ = u_k b_k^+ - v_k a_k. \tag{8}$$

Where u_k and v_k are real functions as follows:

$$u_k^2 - v_k^2 = 1. \tag{9}$$

Inverse transform of Eq. (8):

$$a_k = u_k\alpha_k + v_k\beta_k^+, \quad a_k^+ = u_k\alpha_k^+ + v_k\beta_k,$$

$$b_k = u_k\beta_k + v_k\alpha_k^+, \quad b_k^+ = u_k\beta_k^+ + v_k\alpha_k. \tag{10}$$

All in Eq. (10) are applied in Eq. (6), we get

$$H = -NA(J_1+J_2)S^2 + \sum_k AS[(J_1+J_2)(u_k^2+v_k^2) + 2(J_1\gamma_k + J_2\gamma'_k)u_k v_k]\alpha_k^+\alpha_k + \sum_k AS[(J_1+J_2)(u_k^2+v_k^2) +$$

$$+ 2(J_1\gamma_k + J_2\gamma'_k)u_k v_k]\beta_k^+\beta_k + \sum_k AS[(J_1\gamma_k + J_2\gamma'_k)(u_k^2+v_k^2) + 2(J_1+J_2)u_k v_k](\alpha_k^+\beta_k^+ + \alpha_k\beta_k) +$$

$$+\sum_k AS[2(J_1+J_2)v_k^2 + 2(J_1\gamma_k + J_2\gamma'_k)u_k v_k]. \tag{11}$$

Diagonalize the above formula:

$$(J_1\gamma_k + J_2\gamma'_k)(u_k^2+v_k^2) + 2(J_1+J_2)u_k v_k = 0. \tag{12}$$

Combine Eq. (9) and Eq. (12), we get

$$v_k^2 = \frac{-1+\Delta}{2}; \quad u_k^2 = \frac{1+\Delta}{2}, \quad \Delta = \sqrt{\frac{w^2}{w^2-4}};$$

$$w = \frac{2(J_1+J_2)}{J_1\gamma_k + J_2\gamma'_k}. \tag{13}$$

Since δ and ε only depend on the coordinate numbers, which are the same for nearest- and the next-nearest-neighbor, while differ only in directions, so we can approximately get $|\gamma_k| \cong |\gamma'_k|$, therefore

$$w = \frac{2(J_1+J_2)}{J_1\gamma_k + J_2\gamma'_k} = \frac{2}{\gamma_k}, \tag{14}$$

$$\Delta = \sqrt{\frac{w^2}{w^2-4}} = \sqrt{\frac{1}{1-\gamma_k^2}}. \tag{15}$$

Combine Eqs. (11), (13) and (15), we have

$$H = -NA(J_1+J_2)S(S+1) +$$

$$+\sum_k A(J_1+J_2)S\sqrt{1-\gamma_k^2}(\alpha_k^+\alpha_k + \beta_k^+\beta_k + 1). \tag{16}$$

If $\hbar\omega_k = A(J_1+J_2)S\sqrt{1-\gamma_k^2}$. Where $\hbar\omega_k$ presents the antiferromagnetic spin-wave quantum, thus

$$H = -NA(J_1+J_2)S(S+1) +$$

$$+\sum_k \hbar\omega_k\left[(\alpha_k^+\alpha_k + \frac{1}{2}) + (\beta_k^+\beta_k + \frac{1}{2})\right]. \tag{17}$$

Evidently, there are two degenerate antiferromagnetic spin waves to each k, with $\alpha^+\alpha$, $\beta^+\beta$ (n_k) as the particle number operators. At lower temperature, we use long-wave conditions ($ka << 1$) to expand γ_k:

$$\gamma_k \approx 1 - \frac{k^2a^2}{A}. \tag{18}$$

The long-wave dispersion relation is

$$\hbar\omega_k = A(J_1+J_2)S\sqrt{1-\left(1-\frac{k^2a^2}{A}\right)^2} \approx$$

$$\approx A(J_1+J_2)S\sqrt{\frac{2k^2a^2}{A}} = \sqrt{2A}(J_1+J_2)Ska. \tag{19}$$

Thus the frequency of the antiferromagnetic spin wave is a linear function of k and identical to the long-wave dispersion of the acoustic phonons. And based on Plunk distribution:

$$< n_k > = < \alpha_k^+\alpha_k > = < \beta_k^+\beta_k > = \frac{1}{\exp(\hbar\omega_k / K_BT) - 1}. \tag{20}$$

Therefore the sum of all magnon n_k is

$$\sum_k < n_k > = \sum_k < \alpha_k^+ \alpha_k > = \sum_k < \beta_k^+ \beta_k > =$$

$$= \sum_k \frac{1}{\exp(\hbar\omega_k / K_B T) - 1} = \frac{V}{(2\pi)^3} \int_0^\infty \frac{4\pi k^2 dk}{\exp(\hbar\omega_k / K_B T) - 1}. \quad (21)$$

In antiferromagnetism, from the excited spin wave quantum we get the internal energy from the magnons under the temperature T:

$$U(T) = \sum_k < \alpha_k^+ \alpha_k >_T \hbar\omega_k + \sum_k < \beta_k^+ \beta_k >_T \hbar\omega_k =$$

$$= 2\sum_k < n_k >_T \hbar\omega_k . \quad (22)$$

Combine Eqs. (19), (21) and (22), we have

$$U(T) = \frac{2Na^3}{8\pi^3} \int_0^\infty \frac{4\pi\hbar\omega_k k^2 dk}{\exp(\hbar\omega_k / K_B T) - 1} =$$

$$= \frac{N(K_B T)^4}{\pi^2 [\sqrt{2A}(J_1 + J_2)S]^3} \zeta(4)\Gamma(4). \quad (23)$$

4. Results and discussions

From Eq. (23) above, therefore, in the lower temperature the specific heat from the magnons is

$$C_m = \frac{\partial U(T)}{\partial T} = \frac{4K_B N(K_B T)^3}{\pi^2 [\sqrt{2A}(J_1 + J_2)S]^3} \zeta(4)\Gamma(4) = \beta T^3. \quad (24)$$

It can be concluded from the above that C_m is proportional to T^3 and the theoretic results are comparable to the experimental data [11], as shown in Fig. 2. Where we take $\Gamma(4) = 6$, $\zeta(4) = \pi^4/90$, $S = 1$, $A = 4$, $J_1 \sim 0.0498$ eV, $J_2 \sim 0.0510$ eV [10], all parameters are applied to Eq. (24), we get $\beta \sim 0.4878$ mJ/(mol·K^4), and this value agrees with the experimental data [23].

For the sake of comparison to other experimental results, we rewrite Eq. (24), and then arrive at

$$\frac{C_m}{T} = \frac{4NK_B^4}{\pi^2 [\sqrt{2A}(J_1 + J_2)S]^3} \zeta(4)\Gamma(4)T^2 = \beta T^2 \propto T^2. \quad (25)$$

Then under zero magnetic fields C_m/T is proportional to T^2 and consistent with experimental measurements [22], as shown in Fig. 3, comparable to other experimental results [4,24].

However, in Fig. 2 we can find that there is a certain morphological difference, especially, when the temperature T is more than 30 K, such a difference originates perhaps from our quasi-two-dimensional analysis and approximate calculations, while the actual Fe-oxide superconductors have three-dimensional lattice, so a certain divergence between theoretical values and experimental data is inevitable.

Although there are slightly some differences between the theoretic results and the experimental data in Figs. 2 and 3, in the lower temperature the specific heat C_m is still proportional to T^3 in Eqs. (24) and (25) applied by many theoretic and experimental parameters. Such a characteristic is easy apprehended in term of the quantization of spin waves. As known well, the quantization of spin waves (magnons) proceeds exactly as for photons and phonons, however, the photons can play hardly any important role in the thermal capacity, thus the specific heat C_m originate basically from the phonons in the lower temperature. Of course, the free electrons can also contribute to the specific heat in the same circumstances. In general, the specific heat of metals may be written as the sum of electron and phonon contributions: $C = \gamma T + AT^3$, where γ and A are constants from the material characteristics. The electronic term is linear in T and becomes an important component of C at sufficiently low temperature, for example, both electron and phonon contributions are comparable at the liquid

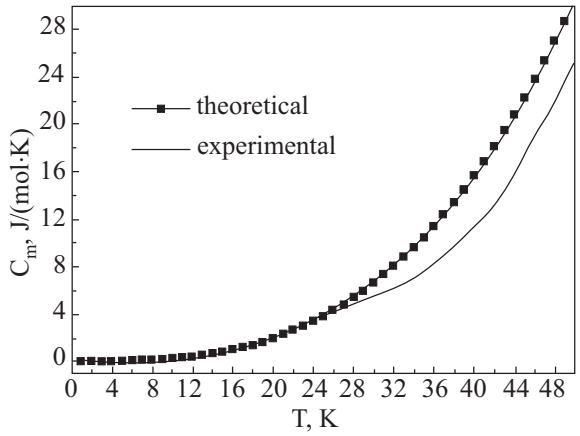

Fig. 2. $C_m \sim T$ relations between the theoretic results are comparable to the experimental data [11].

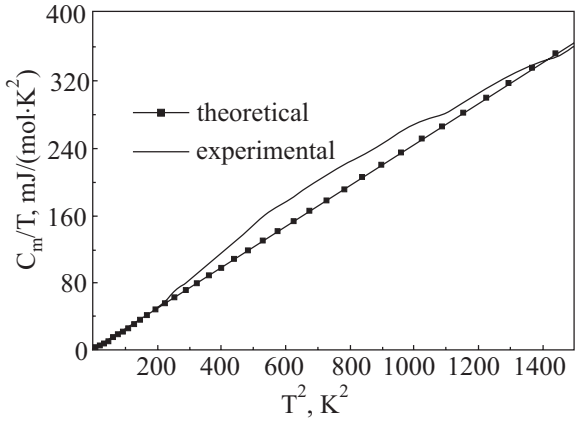

Fig. 3. $C_m/T \sim T^2$ relations between the theoretical calculations and experimental measurements [23].

helium temperature. However, in Fe-oxide superconductors, the density of free electrons is so small that the electronic term should hardly play any role in the specific heat, because the electron (carrier) density at 100 K is only $9.8 \cdot 10^{20}/\text{cm}^3$, which is close to the cuprate superconductors [25,26]. Such a density is much less than the electron density of metals, which is known about $10^{23}/\text{cm}^3$, therefore, the electron contributions in Fe-oxide superconductors may not approach to 1% ones in the metals even at the liquid helium temperature. In practice, it is difficult to distinguish less than 1% and even smaller the specific heat quantities in the experiments. From the analysis above we understand the phonon contribution to the specific heat should be suitable as the T^3 law in Eq. (24).

Significantly, the relation of $C_m \propto T^3$ from the magnons in the antiferromagnetic compounds is similar to that from Debye phonons in the general solids, nevertheless, Debye T^3 law is only appropriate to the experimental results in the very low temperature, for instance, below $T = \Theta_D/50$. Generally, the Θ_D of Fe-based AFM material is about 400 K [27] (and its $\beta \sim 0.464$ mJ/(mol·K^4) is close to here $\beta \sim 0.4878$ mJ/(mol·K^4) as above), then $\Theta_D/50$ is about 8 K, that is to say Debye T^3 law is only valid under so low temperature. Moreover, Ref. 27 suggested the C originates from a typical spin-wave contribution for an AFM material. In contrast with Debye T^3 law, here the relation of $C_m \propto T^3$ law in Fe-oxide superconductors accords with the experimental data for T from 0 to 30 K as shown in Fig. 2. So the magnon is the most important contribution from 8 to 30 K. Furthermore, when the T is over 30 K, in the low temperature the spontaneous magnetic susceptibility in the ferromagnetic materials may be expressed as the known Bloch's $T^{3/2}$ law, which originates likewise from the magnon and even the phonon contributions and is analogous to the T^3 law of the specific heat in the antiferromagnetic compounds in the quantization of spin waves.

In summary of the above, under long wave approximation it is concluded that the physical attributes of Fe-oxide superconductors, such as the internal energy and specific heat, still accord with classical theory. However, the superconductivity of Fe-oxide compounds can not be reasonably explained in terms of the thermal properties, which need further discussions in the future researches.

5. Conclusion

In conclusions, based on the structure characteristics of magnetic order from the experiments concerning Fe-oxide superconductors, we applied Heisenberg interaction model and analyzed systematically the antiferromagnetic configuration with the spin-density-wave to suggest the analytic expressions of internal energy and specific heat under the long-wave conditions through the strictly mathematical-physical derivation. Our analytic values show good consistence with the experimental results, therefore, the spin density wave theory can properly describe the physical characteristics of Fe-oxide superconductors. At the same time, the above theory can be also applied to the study of the zero-point energy, magnetic susceptibility, thermal conductivity, Hall coefficient and other important physical quantities, which will be discussed in our future researches.

This work is supported by The Natural Science Foundation of China (No. 10647145).

1. Y. Kamihara, T. Watanabe, M. Hirano, and H. Hosono, *J. Am. Chem. Soc*. **130**, 3296 (2008).
2. H. Takahashi, K. Igawa, K. Arii, Y. Kamihara, M. Hirano, and H. Hosono, *Nature* (*London*) **453**, 376 (2008).
3. X.H. Chen, T. Wu, G. Wu, R.H. Liu, H. Chen, and D.F. Fang, *Nature* (*London*) **453**, 761 (2008).
4. G.F. Chen, Z. Li, D. Wu, G. Li, W. Z. Hu, J. Dong, P. Zheng, J.L. Luo, and N.L. Wang, *Phys. Rev. Lett.* **100**, 247002 (2008).
5. Z.A. Ren, J. Yang, W. Lu, W. Yi, G.C. Che, X.L. Dong, L.L. Sun, and Z.X. Zhao, *Europhys. Lett*. **82**, 57002 (2008).
6. Z.A. Ren, J. Yang, W. Lu, W. Yi, G.C. Che, X.L. Dong, L.L. Sun, and Z.X. Zhao, *Mater. Res. Innovations* **12**, 105 (2008).
7. Z.A. Ren, J. Yang, W. Lu, W. Yi, X.L. Shen, Z. Cai, G.C. Che, X.L. Dong, L.L. Sun, F. Zhou, and Z.X. Zhao, *Chin. Phys. Lett*. **25**, 2215 (2008).
8. R.H. Liu, G. Wu, T. Wu, D.F. Fang, H. Chen, S.Y. Li, K. Liu, Y.L. Xie, X.F. Wang, R.L. Yang, L. Ding, C. He, D.L. Feng, and X.H. Chen, *Phys. Rev. Lett*. **101**, 087001 (2008).
9. Z.A. Ren, J. Yang, W. Lu, W. Yi, X.L. Shen, Z. Cai, G.C. Che, X.L. Dong, L.L. Sun, F. Zhou, and Z.X. Zhao, *Europhys. Lett*. **83**, 17002 (2008).
10. F. Ma, Z.Y. Lu, and T. Xiang, *Phys. Rev*. **B78**, 224517 (2008).
11. J. Dong, H.J. Zhang, G. Xu, Z. Li, G. Li, W.Z. Hu, D. Wu, G.F. Chen, X. Dai, J.L. Luo, Z. Fang, and N.L. Wang, *Europhys. Lett*. **83**, 27006 (2008).
12. T. Yildirim, *Phys. Rev. Lett*. **101**, 057010 (2008).
13. Z.P. Yin, S. Lebegue, M.J. Han, B.P. Neal, S.Y. Savrasov, and W.E. Pickett, *Phys. Rev. Lett*. **101**, 047001 (2008).
14. C. de la Cruz, Q. Huang, J.W. Lynn, J. Li, W. Ratcliff, J.L. Zarestky, H.A. Mook, G.F. Chen, J.L. Luo, N.L. Wang, and P. Dai, *Nature* (*London*) **453**, 899 (2008).
15. A. Wang, X. Wang, Y. Cao, X. Li, Y. Wang, L. Gao, H. Lu, J. Zhang, and P. Li, *Fiz. Nizk. Temp*. **34**, 219 (2008) [*Low Temp. Phys*. **34**, 168 (2008)].
16. I.I. Mazin, D.J. Singh, M.D. Johannes, and M.H. Du, *Phys. Rev. Lett.* **101**, 057003 (2008).
17. D.X. Yao and E.W. Carlson, *Phys. Rev*. **B78**, 052507 (2008).
18. G.S. Uhrig, M. Holt, J. Oitmaa, O.P. Sushkov, and R.R.P. Singh, *Phys. Rev*. **B79**, 092416 (2009).
19. V.G. Bar'yakhtar, *Theoretical and Mathematical Physics*, Springer, New York, **53**, 1047 (1982).
20. D.A. Ivanov and M.A. Skvortsov, *J. Phys. A: Math. Theory* **41**, 215003 (2008).

21. M.J. Skrinjar, D.V. Kapor, and S.D. Stojanovic, *J. Phys.: Condens. Matter* **1**, 725 (1989).
22. Z.Z. Li, *Solid State Theory*, Higher Education Press in Chinese (2002), p. 77.
23. G. Mu, X.Y. Zhu, L. Fang, L. Shan, C. Ren, and H.H. Wen, *Chin. Phys. Lett*. **25**, 2221 (2008).
24. Z. Li, G.F. Chen, J. Dong, G. Li, W. Hu, D. Wu, S. Su, P. Zheng, T. Xiang, N. Wang, and J. Luo, *Phys. Rev*. **B78**, 060504(R) (2008).
25. X.Y. Zhu, F. Han, G. Mu, B. Zeng, P. Cheng, B. Shen, and H.H. Wen, *Phys. Rev*. **B79**, 024516 (2009).
26. G.F. Chen, W.Z. Hu, J.L. Luo, and N.L. Wang, *Phys. Rev. Lett*. **102**, 227004 (2009).
27. I. Felner, I. Nowik, U. Yaron, O. Cohen, E.R. Bauminger, T. Kroener, and G. Czjzek, *Phys. Rev.* **B48**, 16040 (1993).